Ceramics International 46 (2020) 5594–5601

Contents lists available at ScienceDirect

Ceramics International

journal homepage: www.elsevier.com/locate/ceramint

Processing and thermal characterization of polymer derived SiCN(O) and SiOC reticulated foams

Balanand Santhosh[a,*], Cekdar Vakifahmetoglu[b], Emanuel Ionescu[c], Andreas Reitz[d], Barbara Albert[d], Gian Domenico Sorarù[a]

[a] Department of Industrial Engineering, University of Trento, via Sommarive 9, 38123, Trento, Italy
[b] Izmir Institute of Technology, Materials Science and Engineering, 35430, Urla, Izmir, Turkey
[c] TU Darmstadt, Institute for Materials Science, Dispersive Solids, Otto-Berndt-Straße 3, D-64287, Darmstadt, Germany
[d] TU Darmstadt, Eduard-Zintl-Institut für Anorganische und Physikalische Chemie, Alarich-Weiss-Straße 12, D-64287, Darmstadt, Germany

ARTICLE INFO

Keywords:
Polymer derived ceramic
SiOC
SiCN(O)
Foams
Thermal conductivity

ABSTRACT

Highly porous polymer-derived SiCN(O) and SiOC ceramics with low thermal conductivity were developed by replicating polyurethane (PU) foams. The PU templates were impregnated with polysilazane or polysiloxane precursor, followed by pyrolysis at different temperatures (1200 °C - 1500 °C) yielding SiCN(O) or SiOC ceramic foams, respectively. The swelling and cross-linking behavior of the used precursors had a significant impact on the morphology of the prepared foams. The samples had bulk densities ranging from 0.03 $g.cm^{-3}$ to 0.56 $g.cm^{-3}$ and a total porosity in the range from 75 to 98 vol%. Fourier transform infrared (FT-IR), Raman spectroscopy, X-ray diffraction (XRD) were employed to follow the structural evolution together with morphological characterization by scanning electron microscopy (SEM). The obtained ceramics were thermally stable up to 1400 °C, and the linear thermal expansion coefficient values of the porous SiCN(O) and SiOC components in the temperature range from 30 to 850 °C were found to be ~1.72 x $10^{-6}.K^{-1}$ and ~1.93 x $10^{-6}.K^{-1}$, respectively. Thermal conductivity (λ) as low as 0.03 $W.m^{-1} K^{-1}$ was measured for the SiCN(O) and SiOC foams at room temperature (RT). The λ of the ceramic struts were also assessed by using the Gibson-Ashby model and estimated to be 2.1 $W.m^{-1} K^{-1}$ for SiCN(O), and 1.8 $W.m^{-1} K^{-1}$ for SiOC.

1. Introduction

In the last decade, porous Si-based ceramics have drawn a great deal of attention for their useful properties in many fields such as energy, environment, etc. [1,2]. Several different processing techniques can be used to fabricate these materials: replica, emulsion, aerogel, sacrificial templating, etc. [3,4] One emerging method to produce porous Si-based ceramics is the "Polymer Derived Ceramic" (PDC) route [5]. Accordingly, highly porous polymer derived ceramics were reported in the literature and they have been found suitable for several applications such as catalysis, filtration, ion encapsulation, drug delivery as well as thermal insulation [6–13].

The mechanical properties, thermal and chemical stability, oxidation resistance and high temperature creep behavior of PDCs have already been studied [14–18]. Nevertheless, the thermal properties are the least investigated property for PDCs. Only recently Gurlo et al. [19] studied the thermal conductivity, λ, for dense bulk hot-pressed SiOC ceramics from RT up to 1000°C; Mazo and co-workers [20,21] determined the λ of spark plasma sintered SiOC materials and Eom et al. [22] reported λ values of SiOC and found that they depend on the processing temperature. Finally, Stabler et al. [23] studied the effect of the phase compositions and microstructures on the thermal properties of SiOC ceramics and found that increasing the amount of precipitated C lead to an increase of λ. While those reports are available for SiOC system, and there are works for the synthesis of porous SiCN ceramics [24–27], to the best of our knowledge the thermal properties of SiCN/SiCN(O) PDCs have been reported very rarely [14,28].

Recently, a replica process was presented to manufacture reticulated SiC foams via the PDC route starting from PU foam impregnated with polycarbosilane [29]. Highly porous ceramic SiC components were characterized by measuring the thermal conductivity at RT which was found to be as low as 0.05 $W.m^{-1} K^{-1}$ for samples with 98% porosity. The aim of this work was to investigate the processing and the thermal properties of reticulated SiCN(O) and SiOC foams. Thermal characterization of polysilazane-derived SiCN(O) materials, as the one reported in this study, should fill a gap in the property set of

* Corresponding author.
E-mail address: balanand.santhosh@unitn.it (B. Santhosh).

https://doi.org/10.1016/j.ceramint.2019.11.003
Received 27 September 2019; Received in revised form 27 October 2019; Accepted 1 November 2019
Available online 03 November 2019

silicon carbonitride materials. Moreover, the study has been performed using two different type of reticulated polyurethane foams: one with fully open and another one with partially closed cells therefore giving the opportunity to evaluate this morphological feature on the thermal properties of the resulting ceramic materials.

Finally, it is well known that is rather difficult to attain SiCN ceramics without any oxygen contamination, which is in part from the impurities in the precursors and also from the oxygen contamination during processing [25,30]. For this reason, we decided to explicitly acknowledge the presence of oxygen in our materials calling these ceramics as SiCN(O).

2. Experimental procedure

2.1. Materials

Commercially available polysilazane, Durazane 1800 (CAS#: 503590-70-3; Merck Performance Materials GmbH, Wiesbaden, Germany, viscosity: < 100 cps at 20 °C) and polysiloxane, SPR-036 (Starfire Systems Inc., NY, USA, viscosity: 50–500 cps at room temperature conditions) were used as the precursors, without any further purification. A Karstedt's catalyst, platinum–divinyltetramethyldisiloxane complex in xylene, having a platinum (Pt) content of ~2% (CAS#: 68478-92-2; Sigma–Aldrich, Saint Louis, MO, USA) was used after further diluting it to a solution having 0.1% of Pt in the xylene (CAS#: 106-42-3, Sigma–Aldrich). Two different types of polyurethane, PU, templates (ARE- S.r.l, Rosate, Milan, Italy) were used for the processing, i.e., MTP-55 (polyester base, partially closed cells, density 0.055 ± 5% $g.cm^{-3}$) and PPI-60 (polyester base, mostly open cells, density 0.025 ± 8% $g.cm^{-3}$).

2.2. Processing

The preceramic foams were prepared upon impregnating PU foams with the commercial preceramic precursors. Acetone (CAS#: 67-64-1; > 99% pure, Sigma–Aldrich) was used as solvent to decrease the viscosity of the polymeric precursors (as low viscosity is favorable for effective swelling of the polymer foam) as well as to provide suitable dissolution and homogeneous mixing of the used Pt catalyst (100 µL of 0.1% Pt solution per 1 g of polymer precursor). The amount of acetone used in the impregnation process was always 1/5th of the volume of PU template. The PU foams of the required dimensions were manually impregnated with this solution system. The process is repeated until visually all the solution has been taken-in by the PU foam, resulting in the swelling of the same. The impregnated PU foam is then left for drying usually for a period of 24 h at room temperature conditions before conducting the pyrolysis. The detailed procedure for the impregnation and preparation of the monolith is reported in Ref. [29] and the process in brief is sketched in Fig. 1.

The pyrolysis was carried out at 1200 °C using a heating rate of 5 °C.min^{-1} and a flow rate of 300 mL.min^{-1} (N_2 was used for SiCN(O) samples, while Ar was used for the SiOC samples) in an alumina tube furnace (Lindberg/Blue, USA), with 5 h of gas purging before starting the heat treatment. Typically, two dwell steps were applied: one at 600 °C for 0.5 h to ensure complete removal of the polyurethane template and another one at the peak temperature lasting 2 h. After the furnace was switched off to allow free cooling to room temperature. Additionally, selected samples were pyrolyzed at higher temperatures, i.e. 1300, 1400 and 1500 °C, using the same treatment conditions (heating rate, flow rate, dwell steps, cooling process) as described above.

Depending on the polyurethane foam used for the fabrication, samples were coded “M”, for those being prepared upon using the MTP-55 as template (having partially closed cells), and “P” for those prepared with PPI-60 template (having only open cells). The ceramic foam samples were made using polyurethane (PU): polymeric precursor (PP) weight ratios of 1:1, 1:2, 1:3, 1:4, 1:5, and 1:6. The information about the used PU: PP ratios was given in the sample codes as well, e.g., the ceramic sample prepared from a mixture with a MTP-55: polysilazane weight ratio of 1 : 4 was named SiCN(O)-M4 or a sample prepared from a mixture with a PPI-60: polysiloxane weight ratio of 1 : 2 was named SiOC–P2. In some cases, the samples were labelled only SiCN(O) and SiOC in order to avoid complications. However, in these cases, it will be clearly mentioned along with the associated text or figure, the details of the sample chosen for that particular study.

2.3. Characterization

The skeletal density measurements were performed using a helium pycnometer (AccuPyc 1330 TC, Micromeritics, Norcross, GA, USA), while the bulk densities were obtained from the respective mass and the geometrical volume of the samples. The thermo-gravimetric analysis (TGA, Netzsch STA 409, Netzsch Gerätebau Gmbh, Selb, Germany) was conducted (1550 °C/N_2 (50 mL.min^{-1})/10 °C.min^{-1}) on the PU templates, the polymeric precursor, the impregnated PU foams and the final ceramic foams. X-ray diffraction (XRD, Rigaku D/Max-B diffractometer, Japan) analysis were collected by using the Cu Kα in 2Θ angle range of 10 to 90°, with a step size of 0.05°, and the data were plotted after normalization. Fourier Transform Infrared (FT-IR, using ATR technique, Varian 4100 FT-IR, Agilent Technologies, Inc., USA) and Raman spectroscopy (Argon laser, wavelength = 514.5 nm, Horiba HR800 micro-Raman spectrometer, Horiba Jobin Yvon GmbH, Bensheim, Germany) were used to evaluate the structural features. The morphology of the samples was studied by Scanning Electron Microscopy (SEM, JEOL JSM 5500 JEOL, Tokyo, Japan). Prior to the measurements, the sample fracture surfaces were sputter-coated with gold in order to avoid charging. The linear expansion coefficients of the ceramic foams were determined using a L75 platinum series dilatometer (Linseis Messgeraete GmbH, Germany) at a heating rate of 5 °C.min^{-1}(with a sample pressure of 150 mN). The C, Si, and, N contents were determined by the Mikroanalytisches Labor Pascher, Germany. For Si determination, the sample is fused in a Pt-crucible with a mixture of Na_2CO_3/H_3BO_3. After dissolution with acids the Si content is measured using an inductively coupled plasma atomic emission spectrometer, ICP-AES, (iCap 6500, Thermo Fisher Scientific, Waltham, Massachusetts, USA). C is measured conductometrically after combustion and adsorption of CO_2 in a 0.1 N NaOH solution. N is measured with a Leco TCH600 analyzer. The amount of oxygen in the ceramic samples was calculated as a difference to 100%. The room temperature (RT) thermal conductivity measurements were performed by using a Hot Disk apparatus (Hot Disk TPS 2500 S, Kagaku Analys AB, Sweden). The thermal diffusivity measurements at high temperatures were conducted on the ceramic foams (only on the ones from the M-type, closed cells, templates) using a Laser Flash LFA 1600 instrument (Linseis

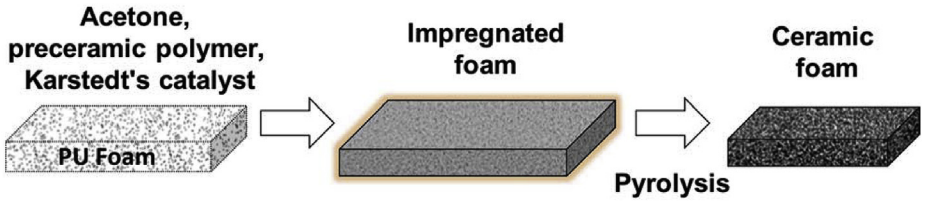

Fig. 1. Process of preparing the sample.

Messgeräte GmbH, Selb, Germany) equipped with a S-type thermocouple. The rationale for using the LFA technique only with the M-type ceramic foams, having partially closed cells, was to avoid problems related to the insufficient absorption of the laser power that we experienced when the same LFA technique was applied to the P-type forms having fully open cells.

3. Results and discussion

3.1. PU templates and precursors

The microstructures of the used PU templates are given in Figs. 2(a & b). As can be seen, the MTP-55 template (M-type) consists partially of closed cells with an average cell size of (580 ± 65) μm, while the cells of PPI-60 (P-type) are completely open porous with larger cells with an average cell size of (920 ± 110) μm.

The FT-IR spectra shown in Fig. 3(a) indicate the presence of characteristic absorption bands for polyurethane at 3295 cm^{-1} (N–H symmetric and asymmetric stretching, absorption band as a shoulder), at 2938 cm^{-1}, 2930 cm^{-1}, and 2864 cm^{-1} (C–H stretching vibrations in methyl and methylene groups), as well as at 1723 cm^{-1} and 1219 cm^{-1} (sharp absorption peaks corresponding to the carboxy groups, i.e. stretching vibration of C═O and asymmetric vibration of C–O, respectively) [24,31]. The TG analysis of both PU foams (see Fig. 3(b)) shows mass loss starting at around 240°C and reaching ca. 90% at temperatures above 450 °C. The FTIR spectra of the preceramic precursors, Durazane 1800 and SPR-036, as well as of the impregnated foams are also shown in Fig. 3(a). In the case of Durazane 1800, characteristic silazane peaks at 3375 cm^{-1} (N–H stretching), 2954 cm^{-1} (C–H stretching), 2126 cm^{-1} (Si–H stretching), 1252 cm^{-1} (C–H deformation), 1163 cm^{-1} (N–H deformation), and ~880 cm^{-1} (Si–N–Si stretching) can be seen [32]. While in the case of polysiloxane precursor, a strong absorption band at ~1100 cm^{-1} corresponding to the Si–O–Si stretching was observed, in addition to a band at ca. 2150 cm^{-1} assigned to Si–H groups [33]. The FT-IR spectra of the impregnated foams still show the Si–H peak which suggest that, as expected, not all the silicon hydrogen bonds have been consumed in the crosslinking reaction via hydrosilylation with the vinyl groups [34,35] since SPR-036 and Durazane 1800 have only few C═C groups available, with a Vy/Si–H molar ratio in the range of 0.1 to 0.2.

The TG curves of the polymer precursors (Durazane 1800, SPR-036, see Fig. 3(b)) show mainly two stages of mass loss. The mass loss in the first stage (below 500 °C) can be attributed to the release of low molecular weight oligomers while in the temperature range between ~ 540 °C and ~ 900 °C, which corresponds to the mineralization stage, mainly methane and hydrogen are released [36–38]. The total mass losses at 1000 °C were ca. 31% and 21% for Durazane 1800 and SPR-036, respectively. The precursor-impregnated PU foams for both M-type and P-type showed, as expected, ceramic yields lying between those of the pure PU templates and of the pure preceramic precursors (Fig. 3(b)).

3.2. SiCN(O) and SiOC foams

SiCN(O) and SiOC ceramic foams with bulk densities ranging from 0.03 $g.cm^{-3}$ to 0.56 $g.cm^{-3}$ were prepared by altering the PU/PP weight ratio (see Fig. 4). As expected, small ratios (i.e. high PP) resulted in relatively high ceramic foam densities; whereas the bulk densities were shown to decrease as the PU/PP ratio increases. The skeletal densities of the prepared ceramic foams were found not to vary significantly and showed values around 2.00 $g.cm^{-3}$. The slight variation in the skeletal densities of the ceramic foams was also correlated to the PU/PP weight ratio, which influences the amount of residual carbon in the samples (resulting from the decomposition of the PU template); consequently, it is expected that an increase of the residual carbon content in the ceramic foams will induce a slight decrease of their density (density of pyrolytic carbon is 1.8 - 2.0 $g.cm^{-3}$ [39] while density of SiCN/SiOC is ca. 2.2 - 2.3 $g.cm^{-3}$ [40,41], see Fig. 4).

It is clear from the micrographs given in Figs. 5(a-h) that the ceramic foams retain the characteristic features of the PU templates. The SiCN(O) and SiOC foams obtained from the M-type PU foam, i.e. the SiCN(O)-M and SiOC-M ceramic foams, exhibit partially closed porosity, while those obtained from P-type foams, i.e. the SiCN(O)–P and SiOC–P ceramic foams show open pores.

Significant difference related to the strut's morphology was observed between the ceramic foam series prepared from Durazane 1800 and SPR-036. The struts were dense for the silazane-derived samples and instead were hollow for the polysiloxane-derived ceramic foams. Such difference probably relates to two features: (i) the better affinity of polyurethane toward polysilazane compared to polysiloxane resulting into a better swelling of PU foam by Durazane[1] and (ii) the different crosslinking kinetics of the polysiloxane and polysilazane precursors, i.e. SPR-036 showing much faster cross-linking than that of Durazane 1800. SPR-036 is thought to have cured on the PU template prior to complete swelling consequently, the ceramic struts are hollow after the PU was burnt out. Indeed, it was already reported that Pt is a very good catalyst for Si–H containing polysiloxane while it is somehow less efficient if the Si–H groups are together with N–H groups such as in the case for polysilazane [42].

The chemical analysis (see Table 1) of the final ceramics was applied to selected samples to understand the effect of the PU/PP weight ratio on the final ceramic composition. The foam type has almost no effect on the final chemical composition, as can be seen by comparing SiOC–P3 and SiOC-M3, which were prepared using the same PU/PP ratio of 1:3. However, the PU/PP weight ratio caused a clear effect on the chemical composition of the ceramic foams, as shown for two SiCN (O) samples in Table 1. The nitrogen content increases with decreasing the PU/PP ratio, since the relative importance of the ceramic residue from PP increases. Similarly, the oxygen contamination increases with increasing the PU/PP ratio, suggesting that such contamination comes more from the decomposition of the PU template during pyrolysis than from the reactivity of the polysilazane with the laboratory atmosphere during the impregnation/curing step.

The XRD patterns of the SiCN(O) and SiOC foams, pyrolyzed at different temperature are shown in Figs. 6(a and c). A hump in the range $20° < 2\Theta < 25°$ shows the presence, for both systems, of an amorphous silica-based phase [20,21] thus confirming, also for the Durazane 1800-derived foams, the presence of oxygen in the SiCN network. The SiCN(O) foams remain amorphous up to 1400 °C while as the pyrolysis temperature is increased to 1500 °C, β-SiC associated reflections around 35.6°, 61.0°, and 71.8° starts to evolve (see Fig. 6(a)). The formation of SiC is due to the well-known decomposition occurring in SiCN-based ceramic systems exposed to temperatures above 1400 °C [43,44]. As for the SiOC system (Fig. 6(c)), the samples remain amorphous up to 1300 °C. At temperatures above 1400°C, the diffraction peaks of β-SiC appear due to partitioning and subsequent carbothermal reaction of the silicon oxy-carbide [29,45,46]. The Raman spectra placed as inset in the XRD plots (see Fig. 6) shows the characteristic disordered (D) and graphitic (G) peaks of the sp^2-hybridized residual carbon up to at least 1400 °C [47,48].

3.3. Thermal studies on SiCN(O) and SiOC foams

The thermal expansion of the foams was studied by dilatometry in the temperature range from 30 to 850 °C, that is the maximum

[1] The submersion of the PU foams into the pure (no solvent) liquid Durazane 1800 and liquid SPR-036 resulted into a volume increase, measured *in situ* in the liquid precursor, of 9.0% and 4.5% respectively unambiguously suggesting that polysilazane has a better affinity compared to polysiloxane for polyurethane.

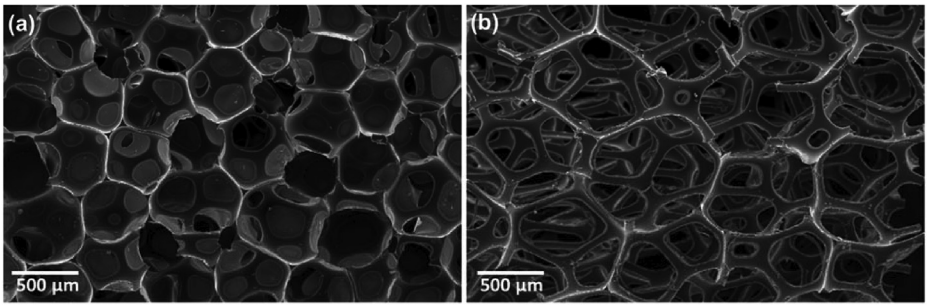

Fig. 2. SEM images of the PU foams (a) MTP-55 (M-type), and (b) PPI-60 (P-type).

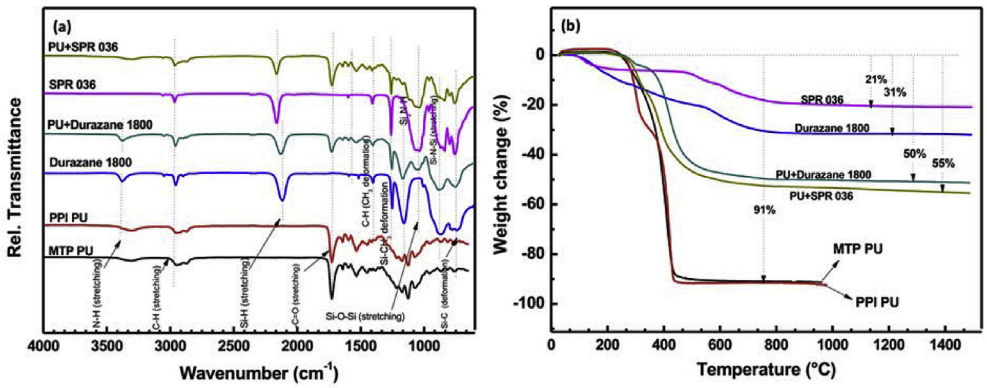

Fig. 3. (a) FTIR spectra of the used PU foams, cross-linked preceramic precursors and the precursor impregnated foams, data for impregnated samples were obtained from M-type foams with 1:2 ratio. (b) TGA data for the PU templates, the pre-ceramic polymer with addition of 100 µL. g^{-1} of Pt catalyst (0.1%) and for the samples prepared from M-type foams impregnated with preceramic polymers in 1:1 wt ratio.

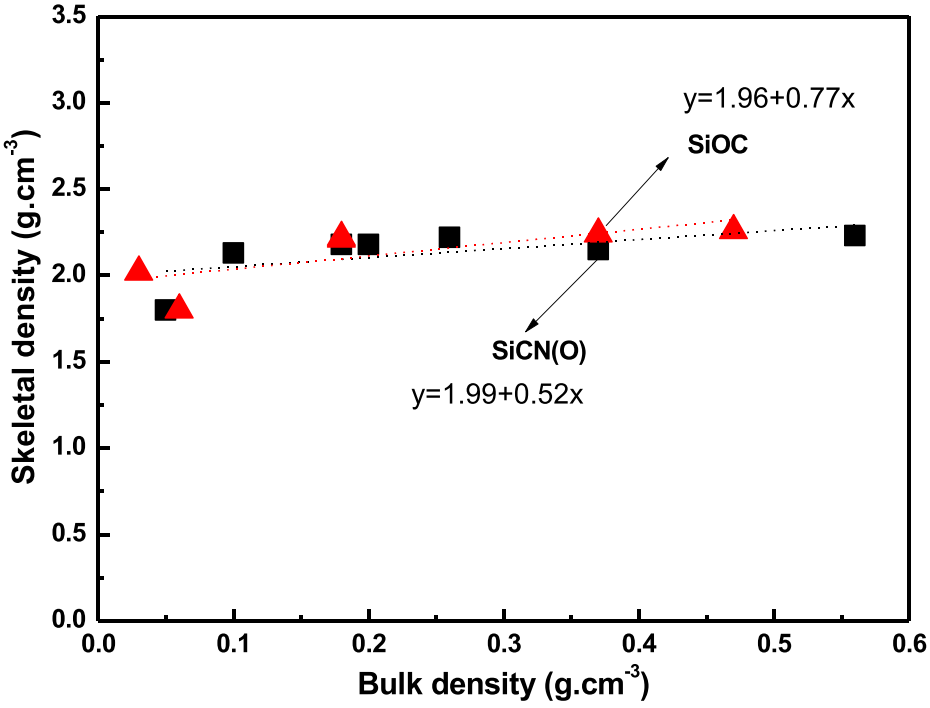

Fig. 4. Skeletal density vs. bulk density of the prepared SiCN(O) and SiOC ceramic foams.

temperature allowed by our dilatometric apparatus. The values of the coefficient of thermal expansion (CTE) were ca. 1.72 x 10^{-6}.K^{-1} and 1.93 x 10^{-6}.K^{-1} for the investigated SiCN(O) and SiOC foams, respectively (Fig. 7(a)). The SiOC sample majorly consists of amorphous silica phase. However, vitreous silica is known to have very low CTE of 0.57 x 10^{-6}.K^{-1} [49]. The reason of an increased CTE value for SiOC, compared to vitreous silica, might be the presence of free carbon and/or nano-crystalline SiC. The observed values were in agreement with recently reported values of dense SiOC ceramics, *e.g.* 1.84-3.23 x 10^{-6}.K^{-1} in the temperature range from 100 to 1000 °C [23]. The measured CTE for the SiCN(O) foam is lower than the value reported in the literature for similar materials (2.69 x 10^{-6}.K^{-1} [28]).

The TG analysis on two ceramic foams up to a temperature of 1600 °C is shown in Fig. 7(b). It can be seen that both the SiOC and SiCN(O) ceramic foams obtained are quite stable up to a temperature of at least 1400 °C, in Ar atmosphere and above 1500 °C the weight loss

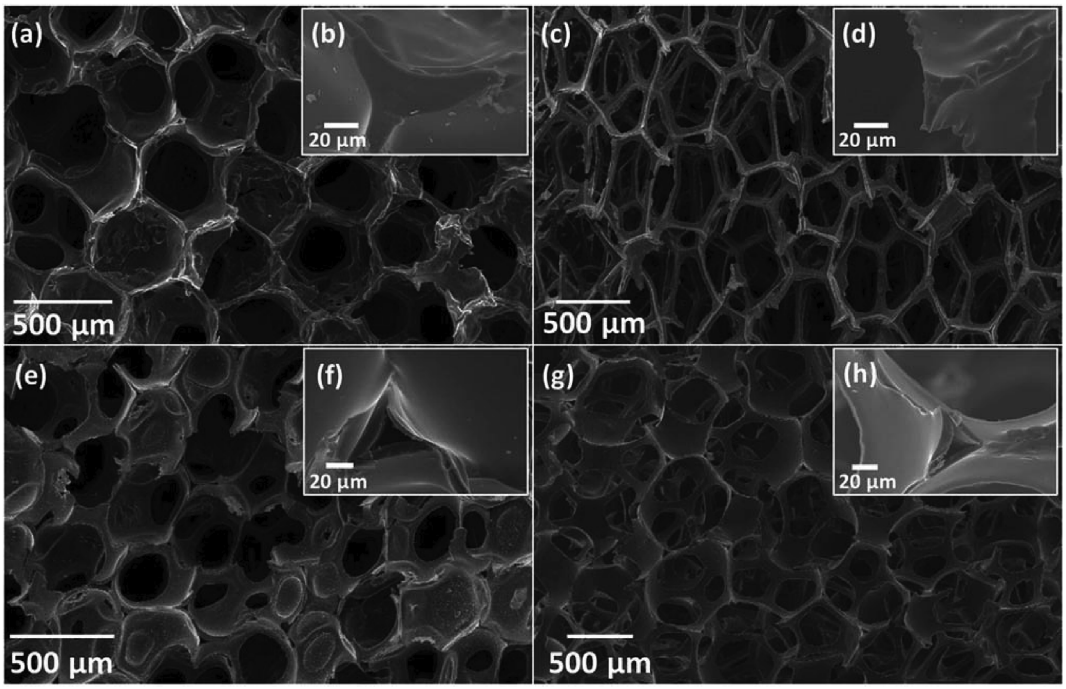

Fig. 5. SEM images of the produced; SiCN(O) ceramic samples (a) SiCN(O)-M2, (c) SiCN(O)–P2; SiOC ceramic samples (e) SiOC-M2, (g) SiOC–P2. (For each image, the insets show the corresponding strut details).

Table 1
Chemical analysis on the SiCN(O) and SiOC foams (from M-type and P-type templates).

Samples	Bulk density (ρ_b ± 0.01) ($g.cm^{-3}$)	Chemical composition (wt.%)			
		Si	C	N	O
SiOC–P3	0.11	43.50 ± 0.4	23.20 ± 0.08	0	33.30 ± 0.3
SiOC-M3	0.24	43.95 ± 0.2	23.36 ± 0.1	0	32.69 ± 0.3
SiCN(O)–P4	0.15	42.25 ± 0.4	26.79 ± 0.06	9.84 ± 0.5	21.13 ± 0.2
SiCN(O)-M6	0.56	47.20 ± 0.3	23.03 ± 0.02	15.35 ± 0.4	14.43 ± 0.1

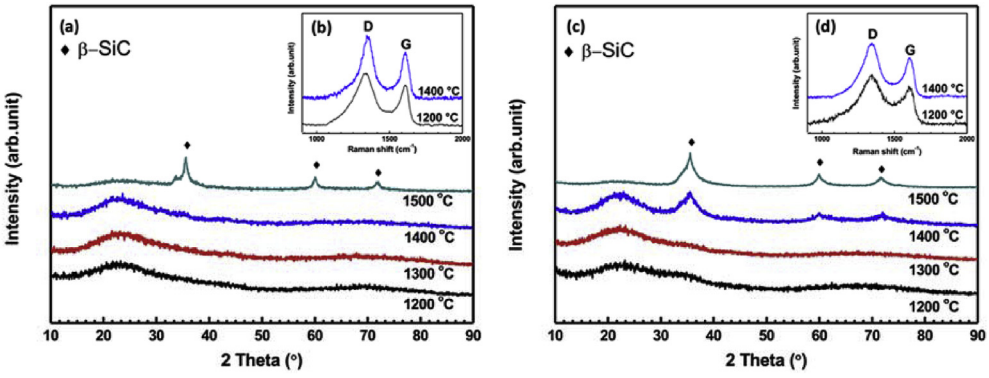

Fig. 6. X-ray diffraction patterns and Raman spectra of SiCN(O)-M2 ((a) and (b), respectively) and of SiOC-M2 ((c) and (d), respectively).

suggests a decomposition process which agrees with the XRD results shown before.

Thermal conductivity measurements were made on all foams produced for which the details are given in Table 2. The bulk density, skeletal density, porosity, and the thermal conductivity values at room temperature of the SiCN(O) and the SiOC are tabulated for each of the samples. The highest bulk density values were found for the M-type foams (partially close cells), for both the polysiloxane and the polysilazane, since the preceramic polymers can impregnate not only the struts but also the walls of the cells. Among the prepared SiCN(O) samples, the highest RT thermal conductivity (λ) was measured for SiCN(O)-M6 (0.20 $W.m^{-1}.K^{-1}$), having a relative density of 0.25 and the lowest was from SiCN(O)–P1 (0.03 $W.m^{-1}.K^{-1}$) sample having a relative density of 0.02. Similar results are shown by the SiOC foams suggesting that the main parameter controlling the TC of the ceramic foams is the density.

With the aim of investigating the influence of the microstructure (open cells vs closed cells) on the TC of the ceramic foam, the experimental data have been plotted as a function of the relative density, differentiating between open vs closed cells (Fig. 8). The data shown in

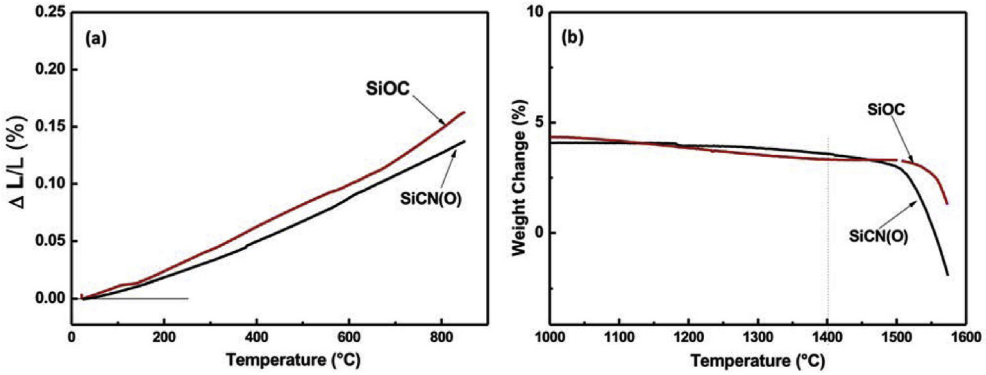

Fig. 7. Dilatometry (a) and TG (b) curves of SiCN(O)-M2 and SiOC-M2.

Fig. 8 reveal that the P-type, open cells PU, in general leads to foams with lower relative density compared to the M-type PU. Indeed, PU foams with partially closed cells, retain more pre-ceramic polymer and form, after pyrolysis, a denser component. However, beside this obvious difference between the two types of templates, the dependence of the TC from the relative density is the same and all the data point, for each chemistry, fall into a master line.

The Gibson-Ashby model for the solid (open cell) foams is given as in equation (1) [50]:

$$\lambda_{Sf} = \frac{1}{3}\left(\frac{\rho_b}{\rho_s}\right)\lambda_S + \left(1 - \frac{\rho_b}{\rho_s}\right)\lambda_{air} \quad (1)$$

This equation can be represented as;

$$\lambda_{Sf} = \left(\frac{1}{3}\lambda_S - \lambda_{air}\right)\frac{\rho_b}{\rho_s} + \lambda_{air} \quad (2)$$

where, λ_{Sf} is the λ of the SiCN(O) or SiOC foam in $W.m^{-1}.K^{-1}$, ρ_b and ρ_s represents the bulk density of the SiCN(O) or SiOC foam and the skeletal density of the SiCN(O) or SiOC ceramics, respectively (given in Table 2, in $g.cm^{-3}$), λ_S is the λ of the SiCN(O) or SiOC ceramic (struts) in $W.m^{-1}.K^{-1}$, and λ_{air} is the λ of air at RT (~0.025 $W.m^{-1}$ K^{-1}). The slope of the linear fit $\left(\frac{1}{3}\lambda_S - \lambda_{air}\right)$ can be used to estimate the λ for dense skeleton. Accordingly, the λ values of the SiCN(O) and SiOC struts evaluated from the Gibson-Ashby model were found to be 2.1 $W.m^{-1}.K^{-1}$ and 1.8 $W.m^{-1}.K^{-1}$, respectively. The values of λ for the silicon oxycarbides struts are consistent with those previously reported in recent literatures for bulk SiOC ceramics, as 1.4 to 1.75 $W.m^{-1}.K^{-1}$ by Gurlo et al. [19], 1.4 to 1.83 $W.m^{-1}.K^{-1}$ in the report by Mazo and co-workers [21], 1.3 to 1.8 $W.m^{-1}.K^{-1}$ by Eom et al. [22], 1.8 to 2.7 $W.m^{-1}K^{-1}$ in the work of Stabler et al. [23], and also with polymer-derived Si–C based ceramics [29]. In case of SiCN(O), to the best of our knowledge, the TC value is the first one reported in the literature, still it falls well in the range of known TC value for the other Si-based PDC materials.

The thermal diffusivity measurements performed from RT up to 1000°C (see Fig. 9), for the SiCN(O) and SiOC ceramic foams prepared from the M-type template. We tried to use the LFA technique also on the P-type open cells foams however, due to insufficient absorption of the laser power of these samples the results were not reliable.

The thermal diffusivity values at RT for SiCN(O) was measured to be 5.9 x 10^{-3} $cm^2.s^{-1}$ and for the SiOC samples 4.8 x 10^{-3} $cm^2.s^{-1}$. Recently, Stabler et al. [23]reported that the thermal diffusivity of dense SiOC obtained after pyrolysis at 1100 °C was ~ 6.75 x 10^{-3} $cm^2.s^{-1}$ at RT and also observed an increase in the diffusivity value with higher pyrolysis temperatures (1600 °C). Similarly, the thermal diffusivity of SiCN ceramics (dense) was reported to increase from 5.07 x 10^{-3} $cm^2.s^{-1}$ to 8.08 x 10^{-3} $cm^2.s^{-1}$ as the treatment temperature was raised from 800 °C to 1300 °C [14]. These reports match well with the diffusivity values measured in this work. As the measurement temperature is raised above 400 °C, there is a gradual increase in the diffusivity values. This could be attributed to the effect of the radiative component [19] in both SiCN (O) and SiOC foams.

4. Conclusions

Polymer derived, reticulated SiCN(O) and SiOC ceramic foams were prepared by replica method; i.e. by impregnating PU foam with Durazane 1800 or SPR 036 preceramic precursors, followed by pyrolysis. The SiCN(O) reticulated ceramic foams from the polysilazane were found to exhibit dense struts, whereas the SiOC ceramic foams prepared with the polysiloxane had hollow struts. This result was related to the different swelling ability of the two Si-precursors in the PU stricture and to their different crosslinking kinetics. The linear thermal expansion coefficient values of the porous SiCN(O) and SiOC foams in

Table 2
The bulk density (ρ_b), skeletal density (ρ_s), porosity, and thermal conductivity (λ) values at RT of SiCN(O) and SiOC ceramic foams pyrolyzed at 1200 °C.

Sample	Bulk density (ρ_b ± 0.01) ($g.cm^{-3}$)	Skeletal density (ρ_s ± 0.1) ($g.cm^{-3}$)	Porosity (%)	Thermal conductivity (λ ± 0.01) ($W.m^{-1}.K^{-1}$)	Sample	Bulk density (ρ_b ± 0.01) ($g.cm^{-3}$)	Skeletal density (ρ_s ± 0.1) ($g.cm^{-3}$)	Porosity (%)	Thermal conductivity (λ ± 0.01) ($W.m^{-1}.K^{-1}$)
SiCN(O)_M1	0.10	2.04	95.1	0.05	SiOC_M1	0.09	2.03	95.6	0.05
SiCN(O)_M2	0.18	2.08	91.3	0.07	SiOC_M2	0.18	2.10	91.4	0.08
SiCN(O)_M3	0.26	2.13	87.8	0.10	SiOC_M3	0.24	2.14	88.8	0.08
SiCN(O)_M4	0.37	2.18	83.0	0.16	SiOC_M4	0.37	2.24	83.5	0.12
SiCN(O)_M5	0.42	2.21	81.0	0.15	SiOC_M5	0.40	2.27	82.4	0.13
SiCN(O)_M6	0.56	2.28	75.4	0.20	SiOC_M6	0.47	2.32	79.7	0.16
SiCN(O)_P1	0.05	2.02	97.5	0.03	SiOC_P1	0.03	1.98	98.5	0.03
SiCN(O)_P2	0.10	2.04	95.1	0.06	SiOC_P2	0.06	2.01	97.0	0.04
SiCN(O)_P3	0.10	2.04	95.1	0.07	SiOC_P3	0.11	2.04	94.6	0.04
SiCN(O)_P4	0.15	2.07	92.8	0.05	SiOC_P4	0.13	2.06	93.7	0.04
SiCN(O)_P5	0.16	2.07	92.3	0.07	SiOC_P5	0.18	2.10	91.4	0.07
SiCN(O)_P6	0.20	2.09	90.4	0.07	SiOC_P6	0.21	2.12	90.1	0.06

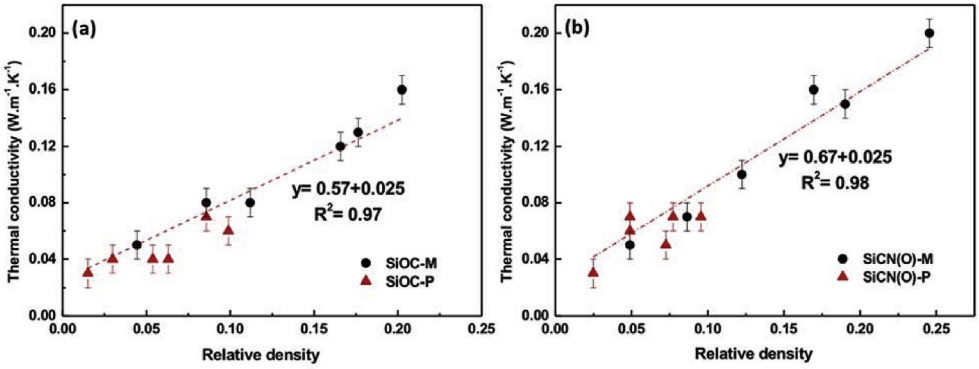

Fig. 8. RT thermal conductivity values measured on the: (a) SiOC and (b) SiCN(O) ceramic foams. Red triangles refer to the open cells, P-type, and black circles to the closed cells, M-type, ceramic foams. (For interpretation of the references to colour in this figure legend, the reader is referred to the Web version of this article.)

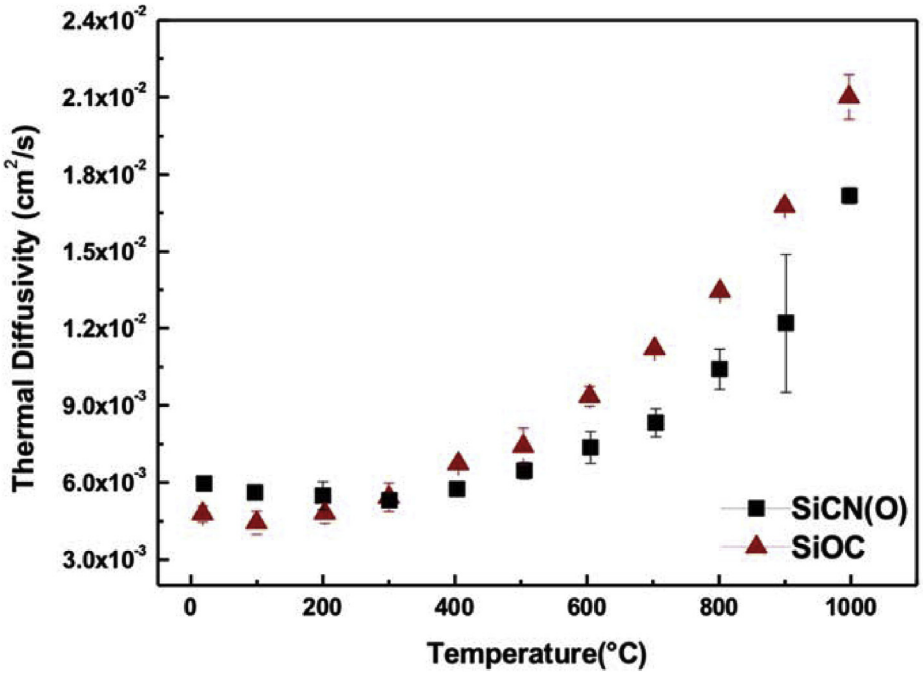

Fig. 9. Thermal diffusivity vs temperature data of SiCN(O)-M2 and SiOC-M2 ceramic foams, by using laser flash technique.

the temperature range from 30 to 850 °C were measured to be ~1.72 x 10^{-6}.K^{-1} and ~1.93 x 10^{-6}.K^{-1}, respectively. The thermal conductivity analysis conducted at room temperature showed that the samples had conductivity in the range from 0.03 $W.m^{-1}$. K^{-1} to 0.20 $W.m^{-1}$. K^{-1} for the SiCN(O) foams, and similarly in the range from 0.03 $W.m^{-1}$. K^{-1} to 0.16 $W.m^{-1}$. K^{-1} for the SiOC foams. A Gibson-Ashby model was used to estimate the thermal conductivity of the ceramic struts (i.e. dense material) which were found to be 2.1 $W.m^{-1}$. K^{-1} for SiCN(O) and 1.8 $W.m^{-1}$. K^{-1} for SiOC. The thermal conductivity of the SiOC ceramic is in line with those already reported in the literature while the one for the SiCN(O) material was never reported before.

Declaration of competing interest

The authors declare that they have no known competing financial interests or personal relationships that could have appeared to influence the work reported in this paper.

References

[1] J.H. Eom, Y.W. Kim, S. Raju, Processing and properties of macroporous silicon carbide ceramics: a review, J. Asian Ceram. Soc. 1 (2013) 220–242, https://doi.org/10.1016/j.jascer.2013.07.003.

[2] K. Lu, Porous and high surface area silicon oxycarbide-based materials - a review, Mater. Sci. Eng. R Rep. 97 (2015) 23–49, https://doi.org/10.1016/j.mser.2015.09.001.

[3] A.R. Studart, U.T. Gonzenbach, E. Tervoort, L.J. Gauckler, Processing routes to macroporous ceramics: a review, J. Am. Ceram. Soc. 89 (2006) 1771–1789, https://doi.org/10.1111/j.1551-2916.2006.01044.x.

[4] T. Ohji, M. Fukushima, Macro-porous ceramics: processing and properties, Int. Mater. Rev. 57 (2012) 115–131, https://doi.org/10.1179/1743280411Y.0000000006.

[5] P. Colombo, G. Mera, R. Riedel, G.D. Sorarù, Polymer-derived ceramics: 40 Years of research and innovation in advanced Ceramics1), Ceram. Sci. Technol. Appl. 4 (2013) 245–320, https://doi.org/10.1002/9783527631971.ch07.

[6] T. Konegger, L.F. Williams, R.K. Bordia, Planar, polysilazane-derived porous ceramic supports for membrane and catalysis applications, J. Am. Ceram. Soc. 98 (2015) 3047–3053, https://doi.org/10.1111/jace.13758.

[7] M.C. Bruzzoniti, M. Appendini, L. Rivoira, B. Onida, M. Del Bubba, P. Jana, G.D. Sorarù, Polymer-derived ceramic aerogels as sorbent materials for the removal of organic dyes from aqueous solutions, J. Am. Ceram. Soc. 101 (2018) 821–830, https://doi.org/10.1111/jace.15241.

[8] M. Fukushima, P. Colombo, Silicon carbide-based foams from direct blowing of polycarbosilane, J. Eur. Ceram. Soc. (2012), https://doi.org/10.1016/j.jeurceramsoc.2011.09.009.

[9] C. Vakifahmetoglu, D. Zeydanli, M.D.D.M. Innocentini, F.D.S. Ribeiro, P.R.O. Lasso, G.D. Soraru, Gradient-hierarchic-aligned porosity SiOC ceramics, Sci. Rep. 7 (2017) 1–12, https://doi.org/10.1038/srep41049.

[10] C. Vakifahmetoglu, M. Buldu, A. Karakuscu, A. Ponzoni, D. Assefa, G.D. Soraru, High surface area carbonous components from emulsion derived SiOC and their gas

sensing behavior, J. Eur. Ceram. Soc. 35 (2015) 4447–4452, https://doi.org/10.1016/j.jeurceramsoc.2015.08.030.
[11] C. Vakifahmetoglu, D. Zeydanli, V.C. Ozalp, B.A. Borsa, G.D. Soraru, Hierarchically porous polymer derived ceramics: a promising platform for multidrug delivery systems, Mater. Des. 140 (2018) 37–44, https://doi.org/10.1016/j.matdes.2017.11.047.
[12] D. Zeydanli, S. Akman, C. Vakifahmetoglu, Polymer-derived ceramic adsorbent for pollutant removal from water, J. Am. Ceram. Soc. 101 (2018) 2258–2265, https://doi.org/10.1111/jace.15423.
[13] V.S. Pradeep, D.G. Ayana, M. Graczyk-Zajac, G.D. Soraru, R. Riedel, High rate capability of SiOC ceramic aerogels with tailored porosity as anode materials for Li-ion batteries, Electrochim. Acta 157 (2015) 41–45, https://doi.org/10.1016/j.electacta.2015.01.088.
[14] N. Janakiraman, F. Aldinger, Fabrication and characterization of fully dense Si-C-N ceramics from a poly(ureamethylvinyl)silazane precursor, J. Eur. Ceram. Soc. 29 (2009) 163–173, https://doi.org/10.1016/j.jeurceramsoc.2008.05.028.
[15] G.D. Sorarù, S. Modena, E. Guadagnino, P. Colombo, J. Egan, C. Pantano, Chemical durability of silicon oxycarbide glasses, J. Am. Ceram. Soc. 85 (2002) 1529–1536, https://doi.org/10.1111/j.1151-2916.2002.tb00308.x.
[16] S. Modena, G.D. Sorarù, Y. Blum, R. Raj, Passive oxidation of an effluent system: the case of polymer-derived SiCO, J. Am. Ceram. Soc. 88 (2005) 339–345, https://doi.org/10.1111/j.1551-2916.2005.00043.x.
[17] R. Riedel, L.M. Ruswisch, L. An, R. Raj, Amorphous silicoboron carbonitride ceramic with very high viscosity at temperatures above 1500°C, J. Am. Ceram. Soc. 81 (1998) 3341–3344, https://doi.org/10.1111/j.1151-2916.1998.tb02780.x.
[18] Y. Wang, Y. Fan, L. Zhang, W. Zhang, L. An, Polymer-derived SiAlCN ceramics resist oxidation at 1400 °C, Scr. Mater. 55 (2006) 295–297, https://doi.org/10.1016/j.scriptamat.2006.05.004.
[19] A. Gurlo, E. Ionescu, R. Riedel, D.R. Clarke, The thermal conductivity of polymer-derived amorphous Si-O-C compounds and nano-composites, J. Am. Ceram. Soc. 99 (2016) 281–285, https://doi.org/10.1111/jace.13947.
[20] M.A. Mazo, C. Palencia, A. Nistal, F. Rubio, J. Rubio, J.L. Oteo, Dense bulk silicon oxycarbide glasses obtained by spark plasma sintering, J. Eur. Ceram. Soc. 32 (2012) 3369–3378, https://doi.org/10.1016/j.jeurceramsoc.2012.03.033.
[21] M.A. Mazo, A. Tamayo, A.C. Caballero, J. Rubio, Electrical and thermal response of silicon oxycarbide materials obtained by spark plasma sintering, J. Eur. Ceram. Soc. 37 (2017) 2011–2020, https://doi.org/10.1016/j.jeurceramsoc.2017.01.003.
[22] J.H. Eom, Y.W. Kim, K.J. Kim, W.S. Seo, Improved electrical and thermal conductivities of polysiloxane-derived silicon oxycarbide ceramics by barium addition, J. Eur. Ceram. Soc. 38 (2018) 487–493, https://doi.org/10.1016/j.jeurceramsoc.2017.09.045.
[23] C. Stabler, A. Reitz, P. Stein, B. Albert, R. Riedel, E. Ionescu, Thermal properties of SiOC glasses and glass ceramics at elevated temperatures, Materials (Basel) 11 (2018) 1–18, https://doi.org/10.3390/ma11020279.
[24] V.L. Nguyen, E. Zera, A. Perolo, R. Campostrini, W. Li, G.D. Sorarù, Synthesis and characterization of polymer-derived SiCN aerogel, J. Eur. Ceram. Soc. 35 (2015) 3295–3302, https://doi.org/10.1016/j.jeurceramsoc.2015.04.018.
[25] W. Zhao, G. Shao, S. Han, C. Cai, X. Liu, M. Sun, H. Wang, X. Li, R. Zhang, L. An, Facile preparation of ultralight polymer-derived SiOCN ceramic aerogels with hierarchical pore structure, J. Am. Ceram. Soc. 102 (2019) 2316–2324, https://doi.org/10.1111/jace.16100.
[26] S.M. Sachau, M. Zaheer, A. Lale, M. Friedrich, C.E. Denner, U.B. Demirci, S. Bernard, G. Motz, R. Kempe, Micro-/Mesoporous platinum–SiCN nanocomposite catalysts (Pt@SiCN): from design to catalytic applications, Chem. Eur J. 22 (2016) 15508–15512, https://doi.org/10.1002/chem.201603266.
[27] P. Jana, O. Santoliquido, A. Ortona, P. Colombo, G.D. Sorarù, Polymer-derived SiCN cellular structures from replica of 3D printed lattices, J. Am. Ceram. Soc. 101 (2018) 2732–2738, https://doi.org/10.1111/jace.15533.
[28] Z.L. Sun, Y. Zhou, D.C. Jia, X.M. Duan, Z.H. Yang, D. Ye, P.F. Zhang, Q. Zhang, Mechanical and thermal physical properties of amorphous SiCN(O) ceramic bulks prepared by hot-press sintering, Mater. Lett. 72 (2012) 57–59, https://doi.org/10.1016/j.matlet.2011.12.053.
[29] P. Jana, E. Zera, G.D. Sorarù, Processing of preceramic polymer to low density silicon carbide foam, Mater. Des. 116 (2017) 278–286, https://doi.org/10.1016/j.matdes.2016.12.010.
[30] R. Michelle Morcos, G. Mera, A. Navrotsky, T. Varga, R. Riedel, F. Poli, K. Müller, Enthalpy of formation of carbon-rich polymer-derived amorphous SiCN ceramics, J. Am. Ceram. Soc. 91 (2008) 3349–3354, https://doi.org/10.1111/j.1551-2916.2008.02626.x.
[31] L. Jiao, H. Xiao, Q. Wang, J. Sun, Thermal degradation characteristics of rigid polyurethane foam and the volatile products analysis with TG-FTIR-MS, Polym. Degrad. Stab. 98 (2013) 2687–2696, https://doi.org/10.1016/j.polymdegradstab.2013.09.032.
[32] P. Furtat, M. Lenz-Leite, E. Ionescu, R.A.F. MacHado, G. Motz, Synthesis of fluorine-modified polysilazanes: via Si-H bond activation and their application as protective hydrophobic coatings, J. Mater. Chem. A. 5 (2017) 25509–25521, https://doi.org/10.1039/c7ta07687h.
[33] M. Wójcik-Bania, A. Łącz, A. Nyczyk-Malinowska, M. Hasik, Poly(methylhydrosiloxane) networks of different structure and content of Si-H groups: physicochemical properties and transformation into silicon oxycarbide ceramics, Polymer (Guildf) 130 (2017) 170–181, https://doi.org/10.1016/j.polymer.2017.10.020.
[34] Y. Blum, G.D. Sorarù, A.P. Ramaswamy, D. Hui, S.M. Carturan, Controlled mesoporosity in SiOC via chemically bonded polymeric “spacers, J. Am. Ceram. Soc. 96 (2013) 2785–2792, https://doi.org/10.1111/jace.12485.
[35] E. Zera, R. Campostrini, P.R. Aravind, Y. Blum, G.D. Sorarù, Novel SiC/C aerogels through pyrolysis of polycarbosilane precursors, Adv. Eng. Mater. 16 (2014) 814–819, https://doi.org/10.1002/adem.201400134.
[36] A. Lavedrine, D. Bahloul, P. Goursat, N. Choong Kwet Yive, R. Corriu, D. Leclerq, H. Mutin, A. Vioux, Pyrolysis of polyvinylsilazane precursors to silicon carbonitride, J. Eur. Ceram. Soc. 8 (1991) 221–227, https://doi.org/10.1016/0955-2219(91)90098-K.
[37] M. Biesuz, P. Bettotti, S. Signorini, M. Bortolotti, R. Campostrini, M. Bahri, O. Ersen, G. Speranza, A. Lale, S. Bernard, G.D. Soraru, First synthesis of silicon nanocrystals in amorphous silicon nitride from a preceramic polymer, Nanotechnology 30 (2019), https://doi.org/10.1088/1361-6528/ab0cc8.
[38] G.D. Sorarù, L. Pederiva, J. Latournerie, R. Raj, Pyrolysis kinetics for the conversion of a polymer into an amorphous silicon oxycarbide ceramic, J. Am. Ceram. Soc. 85 (2002) 2181–2187, https://doi.org/10.1111/j.1151-2916.2002.tb00432.x.
[39] J. Yin, S.H. Lee, L. Feng, Y. Zhu, X. Liu, Z. Huang, S.Y. Kim, I.S. Han, The effects of SiC precursors on the microstructures and mechanical properties of SiC f/SiC composites prepared via polymer impregnation and pyrolysis process, Ceram. Int. 41 (2015) 4145–4153, https://doi.org/10.1016/j.ceramint.2014.11.112.
[40] S.R. Shah, R. Raj, Mechanical properties of a fully dense polymer derived ceramic made by a novel pressure casting process, Acta Mater. 50 (2002) 4093–4103, https://doi.org/10.1016/S1359-6454(02)00206-9.
[41] G.D. Sorarù, L. Kundanati, B. Santhosh, N. Pugno, Influence of free carbon on the Young’s modulus and hardness of polymer-derived silicon oxycarbide glasses, J. Am. Ceram. Soc. 102 (2019) 907–913, https://doi.org/10.1111/jace.16131.
[42] Z. Pan, M. Liu, C. Zheng, D. Gao, W. Huang, Study of karstedt’s catalyst for hydrosilylation of a wide variety of functionalized alkenes with triethoxysilane and trimethoxysilane, Chin. J. Chem. 35 (2017) 1227–1230, https://doi.org/10.1002/cjoc.201700024.
[43] R. Riedel, G. Mera, R. Hauser, A. Klonczynski, Silicon-based polyemr-derived ceramics:synthesis properties and applications-E review, J. Ceram. Soc. Japan. 444 (2006) 33–38.
[44] V.L. Nguyen, N.B. Laidani, G.D. Sorarù, N-doped polymer-derived Si(N)OC: the role of the N-containing precursor, J. Mater. Res. 30 (2015) 770–781, https://doi.org/10.1557/jmr.2015.44.
[45] G.T. Burns, R.B. Taylor, Y. Xu, A. Zangvil, G.A. Zank, High-temperature chemistry of the conversion of siloxanes to silicon carbide, Chem. Mater. 4 (1992) 1313–1323, https://doi.org/10.1021/cm00024a035.
[46] H. Brequel, J. Parmentier, S. Walter, R. Badheka, G. Trimmel, S. Masse, J. Latournerie, P. Dempsey, C. Turquat, A. Desmartin-Chomel, L. Le Neindre-Prum, U.A. Jayasooriya, D. Hourlier, H.-J. Kleebe, G.D. Sorarù, S. Enzo, F. Babonneau, Systematic structural characterization of the high-temperature behavior of nearly stoichiometric silicon oxycarbide glasses, Chem. Mater. 16 (2004) 2585–2598.
[47] J. Ferrari, A. C, Robertson, Interpretation of Raman spectra of disordered and amorphous carbon, Phys. Rev. B. 61, Phys. Rev. B 61 (20) (2000) 14095–14107, https://doi.org/10.1103/physrevb.61.14095 14095–14107. doi:10.1007/BF02543693.
[48] S. Trassl, G. Motz, E. Rössler, G. Ziegler, Characterization of the free-carbon phase in precursor-derived Si-C-N ceramics: I, spectroscopic methods, J. Am. Ceram. Soc. 85 (2002) 239–244, https://doi.org/10.1111/j.1151-2916.2002.tb00072.x.
[49] T. Rouxel, G. Massouras, G.D. Sorarù, High temperature behavior of a gel-derived SiOC glass: elasticity and viscosity, J. Sol-Gel Sci. Technol. 14 (1999) 87–94, https://doi.org/10.1023/A:1008779915809.
[50] L.J. Gibson, M.F. Ashby, Cellular Solids: Structure and Properties, (1997).